Published in final edited form as:
Curr Biol. 2014 October 20; 24(20): 2471–2479. doi:10.1016/j.cub.2014.09.017.

Rapid Glucose Depletion Immobilizes Active Myosin-V on Stabilized Actin Cables

Li Xu[1] and **Anthony Bretscher**[1,2]

[1]Department of Molecular Biology and Genetics, Weill Institute for Cell and Molecular Biology, Cornell University, Ithaca, NY 14853, U.S.A

Summary

Polarization of eukaryotic cells requires organelles and protein complexes to be transported to their proper destinations along the cytoskeleton [1]. When nutrients are abundant, budding yeast grows rapidly transporting secretory vesicles for localized growth and actively segregating organelles [2, 3]. This is mediated by myosin-Vs transporting cargos along F-actin bundles known as actin cables [4]. Actin cables are dynamic structures regulated by assembly, stabilization and disassembly [5]. Polarized growth and actin filament dynamics consume energy. For most organisms, glucose is the preferred energy source and generally represses alternative carbon source usage [6]. Thus upon abrupt glucose depletion, yeast shuts down pathways consuming large amounts of energy, including the vacuolar-ATPase [7, 8], translation [9] and phosphoinositide metabolism [10]. Here we show that glucose withdrawal rapidly (<1 min) depletes ATP levels and the yeast myosin V, Myo2, responds by relocalizing to actin cables, making it the fastest response documented. Myo2 immobilized on cables releases its secretory cargo, defining a new rigor-like state of a myosin-V *in vivo*. Only actively transporting Myo2 can be converted to the rigor-like state. Glucose depletion has differential effects on the actin cytoskeleton resulting in disassembly of actin patches with concomitant inhibition of endocytosis, and strong stabilization of actin cables, thereby revealing a selective and previously unappreciated ATP requirement for actin cable disassembly. A similar response is seen in HeLa cells to ATP depletion. These findings reveal a new fast-acting energy conservation strategy halting growth by immobilizing myosin-V in a newly described state on selectively stabilized actin cables.

Results and Discussion

Myo2 relocalizes rapidly to actin cables in response to glucose depletion

In rapidly growing yeast, Myo2 transports secretory vesicles to sites of cell growth before being deactivated for another cycle of delivery [11]. As a result Myo2-GFP is seen enriched in the buds of growing cells (Figure 1A). However, when cells growing in synthetic complete medium (SC) containing 2% glucose were transferred to water, Myo2-GFP

[2]Author for correspondence: apb5@cornell.edu.

redistributed within 1 min to form fiber-like structures (Figure S1A). Myo2 also redistributed when cells were shifted to SC lacking glucose (Figure 1A and Movie S1) and repolarized rapidly upon glucose restoration (Figures 1A, S1A and Movie S1). Additionally, the redistribution of Myo2-GFP is glucose level dependent (Figures S1B and S1C). Double label and latrunculin (LatA) sensitivity shows that Myo2 is redistributed to actin cables upon glucose deprivation (Figures 1B and 1C). When cells were transferred from SC containing 2% glucose to SC containing 2% galactose, Myo2 relocalized to actin fibers within 1 min (Figure 1D). However, when cells were grown in medium containing 2% galactose, Myo2 was still polarized after galactose depletion (Figure 1E). Under all conditions tested, when Myo2 relocalized to fibers, these corresponded to actin cables (Figures S1D and S1E). Thus, Myo2 relocalization to actin cables is a specific and very rapid response to deprivation of glucose.

Yeast cells respond to glucose depletion in two distinct ways. First, glucose repression/derepression regulates many downstream effectors at transcriptional, and more rapidly, at post-translational levels [6], with the activity and localization of some proteins being regulated by phosphorylation within 5 min after glucose deprivation [12, 13]. Myo2 redistributed upon glucose deprivation in cells lacking the glucose sensor Gpr1 or the suppressor Bcy1, ruling out regulation by the cAMP pathway (Figure S1F). Second, glycolysis provides metabolites and ATP, so glucose depletion is likely to lower ATP levels before alternative carbon sources can be metabolized. To further determine which of these effects contributed to Myo2-GFP relocalization, we used the analog 2-deoxyglucose (2-DG) that is transported into cells, becomes phosphorylated by hexokinase, and causes glucose repression but cannot be further broken down by glycolysis to yield ATP [14] (Figure 2A). When cells were transferred from SC with 2% glucose to SC with 2% 2-DG, Myo2-GFP redistributed to actin cables within 1 min (Figure 2B), indicating that Myo2-GFP relocalization is not due to glucose derepression. Moreover, Myo2-GFP redistributed when cells were transferred to 0.5% glucose and 1.5% 2-DG, but remained polarized in medium with just 0.5% glucose (Figure S1G). Since 2-DG is phosphorylated at the expense of ATP, and 2-DG-6-phosphate is a competitive inhibitor of glucose-6-phosphate for phosphoglucose isomerase, addition of 2-DG rapidly shuts down the glycolytic supply of ATP. Our results show that Myo2-GFP redistribution upon glucose depletion correlates with a reduction in ATP supply. The state of Myo2 visualized upon rapid glucose depletion has not previously been seen and provides a simple assay for the specific and rapid non-transcriptional response to sudden glucose depletion.

Myo2 localization correlates with intracellular ATP level

In cells abruptly depleted of glucose, or switched from glucose to galactose, ATP levels dropped more than 80% within 2 min, whereas when cells growing in galactose were deprived of this carbon source, ATP dropped less than 40% (Figures 2C and S1H). In *hxk2*Δ cells, lacking the major glucose kinase, ATP dropped less than 40% during the 15-min time period following glucose depletion, and Myo2-GFP remained polarized (Figures S1I and S1J). Therefore, Myo2-GFP relocalization to actin cables correlates with a drop in the intracellular ATP level.

After the initial drop of ATP upon glucose depletion, ATP is gradually restored to 50% of its previous level over the next 15 min. This result paralleled the release of Myo2-GFP from cables to gradually become diffuse in the cytoplasm within 30 min after glucose depletion (Figure 2D), while actin cables were still present (Figure S1K). In cells transferred to medium containing 2% 2-DG, the ATP level remained less than 5% of its pre-shift level (Figure 2C) and Myo2 remained associated with actin cables for at least 50 min (Figure 2D). Thus Myo2 dissociates from actin cables when the ATP level recovers.

Where does the ATP come from after glucose depletion? A likely source is by utilization of reserve glycogen or trehalose [15]. In cells unable to utilize trehalose by deletion of the trehalase enzyme (*nth1*Δ), recovery of ATP levels following glucose depletion was unaffected (Figure 2E). By contrast, cells lacking glycogen phosphorylase (*gph1*Δ), that cannot utilize stored glycogen, or in *gsy1*Δ*gsy2*Δ cells, that cannot accumulate glycogen due to the absence of glycogen synthases (Figure 2A), ATP levels hardly showed any recovery over 15 min (Figure 2E). Thus, ATP is restored by utilization of glycogen after the depletion of extracellular glucose.

To test directly how ATP levels affect the localization of Myo2-GFP, we developed a cell model to experimentally manipulate cytosolic ATP. Myo2-GFP remained polarized in yeast cells permeabilized with 0.01% digitonin in SC supplemented with 15 mM ATP. When permeabilized yeast cells were switched to glucose-depleted medium with 15 mM ATP, Myo2-GFP was still polarized (Figures 2F and 2G). However, when both ATP and glucose were depleted, Myo2-GFP redistributed to cables within 1 min (Figures 2F–H). After redistribution to cables by ATP depletion in the permeabilized cell model, Myo2-GFP is repolarized to the bud upon subsequent addition of 15 mM ATP (Figures 2F and 2G). Therefore, Myo2-GFP localization is directly regulated by the intracellular ATP concentration.

Glucose depletion converts myosin-Vs to a rigor-like state with dissociation of secretory vesicle cargo

Myosin family members share a similar mechanism of ATP hydrolysis, actin binding and force transduction, so we examined the effect of glucose depletion on the other myosins in yeast. The class I myosins, Myo3 and Myo5, involved in endocytosis [16], and the single class II myosin, Myo1, involved in cytokinesis [17], did not redistribute upon glucose deprivation, whereas the class V myosin, Myo4, involved in polarized transport of cargos [18] redistributed to cables like Myo2 (Figure S1L). Thus, myosin Vs, but not other yeast myosins, relocalize to actin cables upon glucose depletion.

When ATP is exhausted, the conventional myosin cross-bridge cycle arrests in a rigor state with the ADP-bound head strongly bound to F-actin. To test if Myo2-GFP bound to the actin cables is in a rigor-like state, we used FRAP (Fluorescence Recovery after Photobleaching) to investigate the dynamics of cable associated Myo2-GFP after glucose depletion. In cells growing in the presence of glucose or shortly after glucose depletion, medium buds were selected and photobleached. The fluorescence of Myo2-GFP recovers quickly in cells containing glucose, while almost no recovery was observed in those deprived of glucose (Figure 3A). In addition, when a bar was photobleached across cable-

bound Myo2-3GFP, the bleached region did not migrate or recover for at least 45 sec (Figure 3B), indicating that in glucose-depleted cells, Myo2 is associated with actin cables in a rigor-like state and that the actin cables are no longer treadmilling.

When Myo2 becomes immobilized on actin cables after glucose depletion, bud-oriented transport of cargos by Myo2 is predicted to stop. Secretory vesicles marked with GFP-Sec4 are highly polarized in rapidly growing cells. Upon glucose depletion, GFP-Sec4 labeled vesicles became depolarized in 3 min, not colocalizing with Myo2 on actin cables but largely free in the cytoplasm (Figure 3C), indicating that relocalized Myo2 is unable to bind secretory vesicles. As a more sensitive test to see if Myo2 releases secretory vesicle cargo upon glucose deprivation, we made use of the conditional exocyst mutant *sec6-4* shifted to the restrictive temperature where secretory vesicles marked by GFP-Sec4 and Myo2 hyper-accumulate [11]. Under these conditions, upon glucose deprivation, GFP-Sec4 is dissociated from Myo2 (Figure 3D). In addition to Sec4, Myo2 interacts with exocyst component Sec15 and trans-Golgi associated Rab Ypt32 [19, 20]. Upon glucose deprivation, Myo2 also dissociates from both of these partners (Figures 3E, 3F and S2A). This release is unlikely to be an indirect effect on GTP levels of the Rabs Ypt32 and Sec4, as similar redistribution is seen in the Sec4 RabGAP mutant *msb3*Δ *msb4*Δ (Figure S2B). Moreover, when growing cells were treated with LatA for 3 min, polarized vesicle transport was also abolished due to the loss of actin cable tracks, but Myo2 was found associated with GFP-Sec4 on secretory vesicles regardless of the presence or absence of glucose (Figure 3C and Movie S2). Thus, the disassociation of secretory vesicles from Myo2 is induced by Myo2 immobilization on actin cables. Additionally, we also examined other essential cargos transported by myosin V. Similarly, Mmr1-GFP, a mitochondrial receptor for Myo2 that is usually polarized with Myo2 at the site of growth, became depolarized and colocalized with mitochondria upon glucose depletion (Figures S2C and S2D). Thus, glucose depletion induces active Myo2 to bind strongly to actin cables and release at least some of its cargos.

The rigor-like state of Myo2 requires prior activation by cargo

Myo2 is activated by binding to secretory cargo and then transports the cargo along actin cables. When the secretory pathway is blocked, as occurs in *sec23-1* cells at the restrictive temperature where export from the endoplasmic reticulum is inhibited, Myo2 is inactive and diffuse in the cytosol [11]. In *sec23-1* cells at 26 °C, Myo2-GFP was polarized to growth sites in the presence of glucose and relocalized to actin cables upon glucose depletion (Figures 3G and 3H). However, after shifting to 35 °C for 45 min, Myo2-GFP was depolarized and failed to associate with actin cables upon glucose depletion (Figures 3G and 3H), showing that only active Myo2 can be relocalized. The inability of Myo2 to associate with cables in the *sec23-1* mutant is not due to a higher ATP level, as the profile of ATP level decrease in *sec23-1* cells is indistinguishable from that in wild type cells (Figure S2E). Additionally, when secretory vesicle formation was disrupted by adding 150 μM brefeldin A for 30 min, Myo2-GFP became depolarized and again failed to associate with actin cables upon glucose withdrawal (Figures S2F and S2G).

To explore this relationship further, we examined the response of the conditional tail mutant *myo2-13* that is defective in binding secretory vesicles at the restrictive temperature and

polarizes to the bud tip because it is constitutively active [11, 21]. After shifting *myo2-13* cells to the restrictive temperature, Myo2-13-GFP formed fibers upon glucose depletion, in the presence (*SEC23)* and absence (*sec23-1)* of secretory vesicles (Figures 3I and 3J). Further, a Myo2 motor mutant *myo2-66*, defective in binding actin cables at the restrictive temperature [22], failed to form fibers after glucose withdrawal at 35 °C (Figures 3K and 3L). By contrast, expression of a Myo2 C-terminal truncation lacking the cargo-binding region formed fibers upon glucose depletion, as did a construct with the motor domain and lacking both the dimerization and cargo binding domains (Figures 3M and 3N). Thus, only active Myo2 can be redistributed to actin cables upon glucose depletion.

In summary, these data now establish three states for myosin-V *in vivo*: 1) an inactive state, which is diffusely localized and free of cargo, 2) an activated state, which is triggered by cargo binding [11] and 3) the new rigor-like state described here, which is immobilized on actin cables having released its secretory vesicle cargo. Importantly, the new rigor-like state is only accessible to myosin-V that is active. The inactive state may correspond to a folded structure as seen for mammalian myosin V where the tail binds the motor domain [23, 24]. Thus, we propose the following molecular mechanism: upon ATP reduction, inactive Myo2 remains cytosolic and does not bind actin cables, whereas active Myo2 relocalizes and binds tightly to actin cables and this induces a conformational change in the tail to release its cargos. It is interesting, and surprising, that inactive Myo2 fails to be converted into a rigor-like state by ATP depletion. The reason could be that inactive Myo2 is stably folded in such a way that the Myo2-ADP state does not have access to actin cables.

ATP depletion disassembles cortical patches and stabilizes actin cables

An additional surprising aspect uncovered upon glucose depletion was the stability of the cables to which Myo2 binds (Figure 3B). A previous study showed that 30 min after glucose depletion, actin cortical patches become depolarized [25], but interpretation of this result is complicated by the partial restoration of ATP levels by this time (Figure 2C). We therefore investigated how actin structures are affected immediately after the acute drop of ATP following glucose depletion. Compared to glucose-replete cells, almost no actin patches are observed immediately upon glucose depletion and the remaining few are much less motile (Figure 4A and Movie S3) and endocytosis of the marker FM4-64 is compromised (Figure 4B). Actin patches recover as ATP is restored (Figure 4A and Movie S3). Similarly, when labeled with Abp1-GFP, an actin patch marker, both density and movement of actin patches were decreased in cells transferred to medium lacking glucose or supplemented with 2-DG (Movie S3). Thus, upon reduction of ATP, the actin associated with endocytosis is disassembled.

In growing cells, actin cables are continually assembled and disassembled, with lifetimes of about 1–2 min [5]. Upon glucose depletion, actin cables are not disassembled but become more prominent (Figures 1B, 4A and S3A). The turnover of cables can be assessed by the addition of 150 μM LatA, with cables disappearing within 3 min in cells growing in glucose. Upon glucose depletion, actin cables are resistant to disassembly in 150 μM LatA (Figures 4C, 4D and S3B). Cells pretreated with LatA were not able to reassemble cables after glucose depletion (Figure S3B). Additionally, actin cable stabilization is not likely due to

glucose signaling pathways, as wild type cells treated with 2-DG (Figure S3B) or *gpr1*Δ or *bcy1*Δ cells depleted of glucose (Figure S3D) all have stable actin cables. Therefore glucose depletion and the associated drop in ATP inhibits the disassembly of actin cables.

To further investigate the mechanisms of actin cable stabilization, we examined protein factors that might be involved. Tropomyosins stabilize actin cables but not patches [4, 26]. After shifting to the restrict temperature for 1 min, no actin cables can be found in growing *tpm1-2 tpm2*Δ cells. When *tpm1-2 tpm2*Δ cells were transferred to medium containing 2% 2-DG for 1 min and then shifted to 35 °C for 5 min, cables were still observed (Figures 4E and 4F), indicating that tropomyosin is not necessary to stabilize cables upon depletion of ATP. Formins specifically nucleate and elongate actin cables, and cables are lost in the conditional *bni1-11 bnr1*Δ cells after a shift to the restrictive temperature for 1 min [27]. After switching to medium containing 2% 2-DG, actin cables can still be observed in *bni1-11 bnr1*Δ cells at 35 °C (Figures 4E and 4F), indicating that actin polymerization is not necessary for cable stabilization. Additionally, it has been shown that myosin Vs contributes to actin cables organization in fission yeast [28]. Since Myo2 is immobilized on actin cables upon glucose depletion, it is possible that Myo2 helps to stabilize them. Therefore, we examined the stability of actin cables in *myo2-66* mutant cells in which Myo2-66 is unable to bind actin at the restrictive temperature. When *myo2-66* cells were transferred to medium containing 2-DG at 35 °C, actin cables were still present and resistant to LatA treatment (Figures S3D and S3E). These data indicate that neither tropomyosins, formins nor Myo2 are required for actin cable stabilization upon glucose depletion.

The actin cytoskeleton is highly dynamic in growing cells, mediated in large part by the severing and depolymerizing activity of cofilin [29]. Moreover, it is known that tropomyosin stabilizes actin cables by competition with cofilin [30]. Thus the finding that rapid glucose depletion disassembles cortical patches yet stabilizes actin cables even in the absence of functional tropomyosin is astonishing. To explore if there may not be sufficient cofilin to disassemble both patches and cables, we examined the effect of enhancing cofilin expression on the presence of cables after glucose depletion. Remarkably, the actin cables are resistant to additional cofilin (Figures S3F and S3G). Thus the stability of actin cables following glucose withdrawal implies that they may be selectively stabilized by some factor, or a normal ATP-dependent disassembly process is inhibited, or both. In any case, the stability of these cables reveals that the present knowledge about actin turnover *in vivo* is quite incomplete.

Next, we explored how glucose depletion affects the dynamics of F-actin in higher eukaryotic cells, such as HeLa cells. As most tumor cells depend heavily on glycolysis as their major energy source [31], we transferred cells to medium containing 2-DG as this condition allows us to deplete intracellular ATP rapidly (Figure 4G). When cells were transferred to medium with 2-DG but no glucose, they initially shrank in size (Figure 4H) and microspikes, labeled with GFP-LifeAct, could be observed at the cell periphery (Figure 4I). Interestingly, actin bundles in these ATP-depleted cells are very stable, as actin filaments were still largely present 30 min after LatA treatment while glucose-replete cells rounded up and most actin bundles disappeared within 10 min after LatA addition (Figure

4I). These data indicate that depletion of ATP stabilizes actin bundles in HeLa cells, just as it does in yeast cells.

Yeast in nature is subject to constant nutritional fluctuations and is highly adapted to survive upon nutrition starvation [32]. We postulate that the rapid response to decreased ATP observed in this study is an adaption to glucose deprivation. Changes in intracellular ATP may contribute to general regulatory mechanisms for energy conservation under starvation conditions. For instance, by immobilizing Myo2 onto actin cables and halting actin cable assembly upon glucose depletion, yeast cells immediately conserve energy normally used for polarized transport. Although ATP levels recovered by >50% after 15 min, Myo2 is still largely depolarized. However, actin patches reappear as ATP recovers, indicating that activation of Myo2 requires a higher intracellular ATP level. Thus we propose that for energy conservation during starvation, only necessary processes are re-activated and have access to the limited ATP available, while nonessential pathways are turned off until the stress is relieved.

Supplementary Material

Refer to Web version on PubMed Central for supplementary material.

Acknowledgments

We are grateful to Dr. Kirk Donovan and Myungjoo Shin for reagents, and these and other members of the Bretscher lab for discussions and reading the manuscript. This work was supported by NIH grant GM39066.

References

1. Goode BL, Drubin DG, Barnes G. Functional cooperation between the microtubule and actin cytoskeletons. Curr Opin Cell Biol. 2000; 12:63–71. [PubMed: 10679357]
2. Pruyne D, Legesse-Miller A, Gao L, Dong Y, Bretscher A. Mechanisms of polarized growth and organelle segregation in yeast. Annu Rev Cell Dev Biol. 2004; 20:559–591. [PubMed: 15473852]
3. Hammer JA 3rd, Sellers JR. Walking to work: roles for class V myosins as cargo transporters. Nat Rev Mol Cell Biol. 2011; 13:13–26. [PubMed: 22146746]
4. Pruyne DW, Schott DH, Bretscher A. Tropomyosin-containing actin cables direct the Myo2p-dependent polarized delivery of secretory vesicles in budding yeast. J Cell Biol. 1998; 143:1931–1945. [PubMed: 9864365]
5. Yang HC, Pon LA. Actin cable dynamics in budding yeast. Proc Natl Acad Sci U S A. 2002; 99:751–756. [PubMed: 11805329]
6. Santangelo GM. Glucose signaling in Saccharomyces cerevisiae. Microbiol Mol Biol Rev. 2006; 70:253–282. [PubMed: 16524925]
7. Parra KJ, Kane PM. Reversible association between the V1 and V0 domains of yeast vacuolar H+-ATPase is an unconventional glucose-induced effect. Mol Cell Biol. 1998; 18:7064–7074. [PubMed: 9819393]
8. Kane PM. Disassembly and reassembly of the yeast vacuolar H(+)-ATPase in vivo. J Biol Chem. 1995; 270:17025–17032. [PubMed: 7622524]
9. Ashe MP, De Long SK, Sachs AB. Glucose depletion rapidly inhibits translation initiation in yeast. Mol Biol Cell. 2000; 11:833–848. [PubMed: 10712503]
10. Faulhammer F, Kanjilal-Kolar S, Knodler A, Lo J, Lee Y, Konrad G, Mayinger P. Growth control of Golgi phosphoinositides by reciprocal localization of sac1 lipid phosphatase and pik1 4-kinase. Traffic. 2007; 8:1554–1567. [PubMed: 17908202]

11. Donovan KW, Bretscher A. Myosin-V is activated by binding secretory cargo and released in coordination with Rab/exocyst function. Dev Cell. 2012; 23:769–781. [PubMed: 23079598]
12. Moriya H, Shimizu-Yoshida Y, Omori A, Iwashita S, Katoh M, Sakai A. Yak1p, a DYRK family kinase, translocates to the nucleus and phosphorylates yeast Pop2p in response to a glucose signal. Genes Dev. 2001; 15:1217–1228. [PubMed: 11358866]
13. Aoh QL, Hung CW, Duncan MC. Energy metabolism regulates clathrin adaptors at the trans-Golgi network and endosomes. Mol Biol Cell. 2013; 24:832–847. [PubMed: 23345590]
14. Zimmermann FK, Scheel I. Mutants of Saccharomyces cerevisiae resistant to carbon catabolite repression. Mol Gen Genet. 1977; 154:75–82. [PubMed: 197390]
15. Wilson WA, Roach PJ, Montero M, Baroja-Fernandez E, Munoz FJ, Eydallin G, Viale AM, Pozueta-Romero J. Regulation of glycogen metabolism in yeast and bacteria. FEMS Microbiol Rev. 2010; 34:952–985. [PubMed: 20412306]
16. Geli MI, Riezman H. Role of type I myosins in receptor-mediated endocytosis in yeast. Science. 1996; 272:533–535. [PubMed: 8614799]
17. Watts FZ, Shiels G, Orr E. The yeast MYO1 gene encoding a myosin-like protein required for cell division. EMBO J. 1987; 6:3499–3505. [PubMed: 3322809]
18. Brown SS. Myosins in yeast. Curr Opin Cell Biol. 1997; 9:44–48. [PubMed: 9013666]
19. Jin Y, Sultana A, Gandhi P, Franklin E, Hamamoto S, Khan AR, Munson M, Schekman R, Weisman LS. Myosin V transports secretory vesicles via a Rab GTPase cascade and interaction with the exocyst complex. Dev Cell. 2011; 21:1156–1170. [PubMed: 22172676]
20. Lipatova Z, Tokarev AA, Jin Y, Mulholland J, Weisman LS, Segev N. Direct interaction between a myosin V motor and the Rab GTPases Ypt31/32 is required for polarized secretion. Mol Biol Cell. 2008; 19:4177–4187. [PubMed: 18653471]
21. Schott D, Ho J, Pruyne D, Bretscher A. The COOH-terminal domain of Myo2p, a yeast myosin V, has a direct role in secretory vesicle targeting. J Cell Biol. 1999; 147:791–808. [PubMed: 10562281]
22. Johnston GC, Prendergast JA, Singer RA. The Saccharomyces cerevisiae MYO2 gene encodes an essential myosin for vectorial transport of vesicles. J Cell Biol. 1991; 113:539–551. [PubMed: 2016335]
23. Liu J, Taylor DW, Krementsova EB, Trybus KM, Taylor KA. Three-dimensional structure of the myosin V inhibited state by cryoelectron tomography. Nature. 2006; 442:208–211. [PubMed: 16625208]
24. Thirumurugan K, Sakamoto T, Hammer JA 3rd, Sellers JR, Knight PJ. The cargo-binding domain regulates structure and activity of myosin 5. Nature. 2006; 442:212–215. [PubMed: 16838021]
25. Uesono Y, Ashe MP, Toh EA. Simultaneous yet independent regulation of actin cytoskeletal organization and translation initiation by glucose in Saccharomyces cerevisiae. Mol Biol Cell. 2004; 15:1544–1556. [PubMed: 14742701]
26. Liu HP, Bretscher A. Purification of tropomyosin from Saccharomyces cerevisiae and identification of related proteins in Schizosaccharomyces and Physarum. Proc Natl Acad Sci U S A. 1989; 86:90–93. [PubMed: 2643110]
27. Evangelista M, Pruyne D, Amberg DC, Boone C, Bretscher A. Formins direct Arp2/3-independent actin filament assembly to polarize cell growth in yeast. Nat Cell Biol. 2002; 4:32–41. [PubMed: 11740490]
28. Lo Presti L, Chang F, Martin SG. Myosin Vs organize actin cables in fission yeast. Mol Biol Cell. 2012; 23:4579–4591. [PubMed: 23051734]
29. Okada K, Ravi H, Smith EM, Goode BL. Aip1 and cofilin promote rapid turnover of yeast actin patches and cables: a coordinated mechanism for severing and capping filaments. Mol Biol Cell. 2006; 17:2855–2868. [PubMed: 16611742]
30. Cooper JA. Actin dynamics: tropomyosin provides stability. Curr Biol. 2002; 12:R523–525. [PubMed: 12176375]
31. Gatenby RA, Gillies RJ. Why do cancers have high aerobic glycolysis? Nat Rev Cancer. 2004; 4:891–899. [PubMed: 15516961]

32. Smets B, Ghillebert R, De Snijder P, Binda M, Swinnen E, De Virgilio C, Winderickx J. Life in the midst of scarcity: adaptations to nutrient availability in Saccharomyces cerevisiae. Curr Genet. 2010; 56:1–32. [PubMed: 20054690]

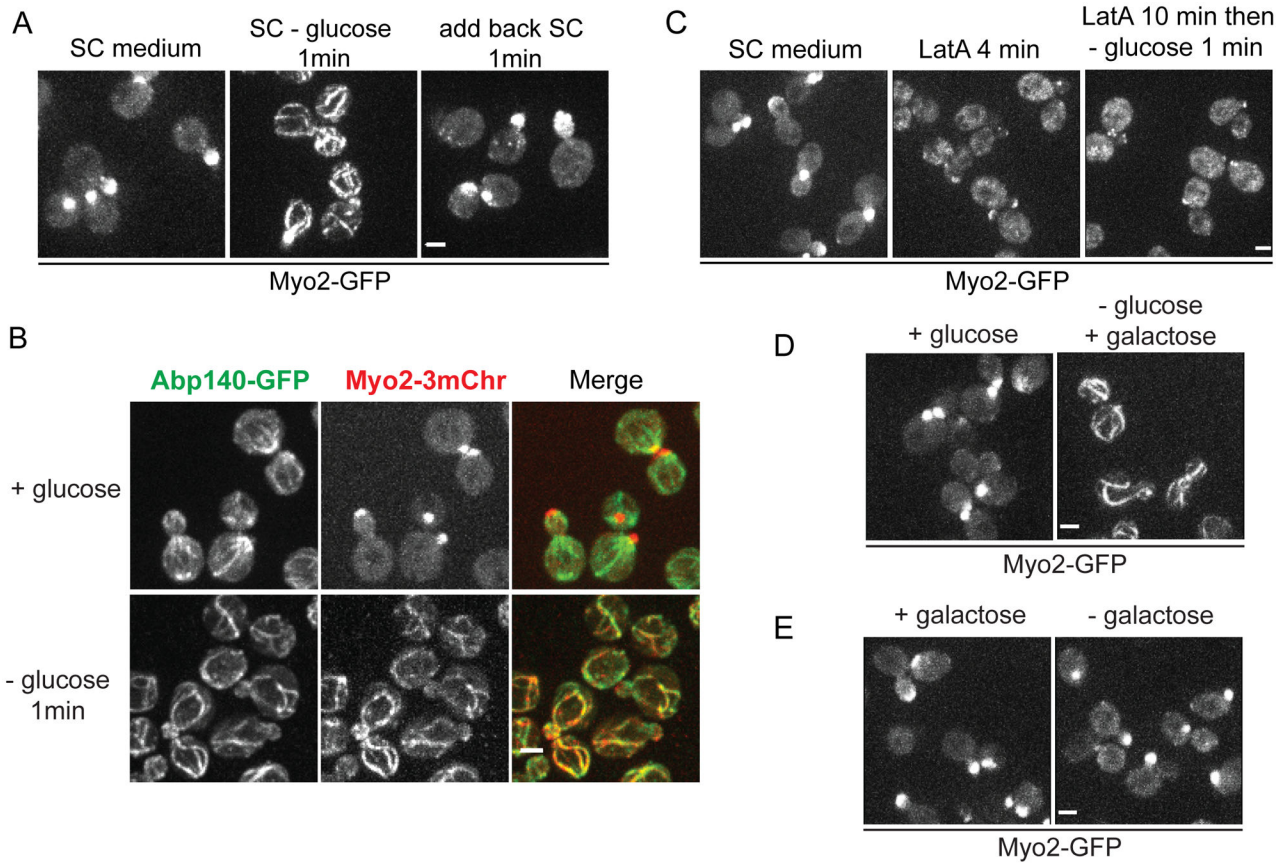

Figure 1. Myo2 relocalizes to actin cables within one minute after glucose depletion

(A) Cells expressing Myo2-GFP grown to mid-log phase in SC were transferred to fresh SC (left) or SC lacking glucose (center), or first transferred into SC lacking glucose for 1 min and then transferred back to SC (right). See also Movie S1.

(B) Cells coexpressing Myo2-3mCherry and Abp140-GFP were transferred to fresh SC or SC lacking glucose for 1 min.

(C) Cells as in (A) transferred to fresh SC (left), SC with 120 μM Latrunculin A (LatA) for 4 min (center), or first transferred to SC with 120 μM LatA for 10 min and then transferred to SC lacking glucose (right).

(D) Cells as in (A) transferred to fresh SC (left) or SC with 2% galactose instead of 2% glucose (right) for 1 min.

(E) Cells were grown overnight in medium with 2% galactose and transferred to fresh medium with 2% galactose (left) or medium lacking a carbon source (right) for 1 min. All scale bars, 2 μm.

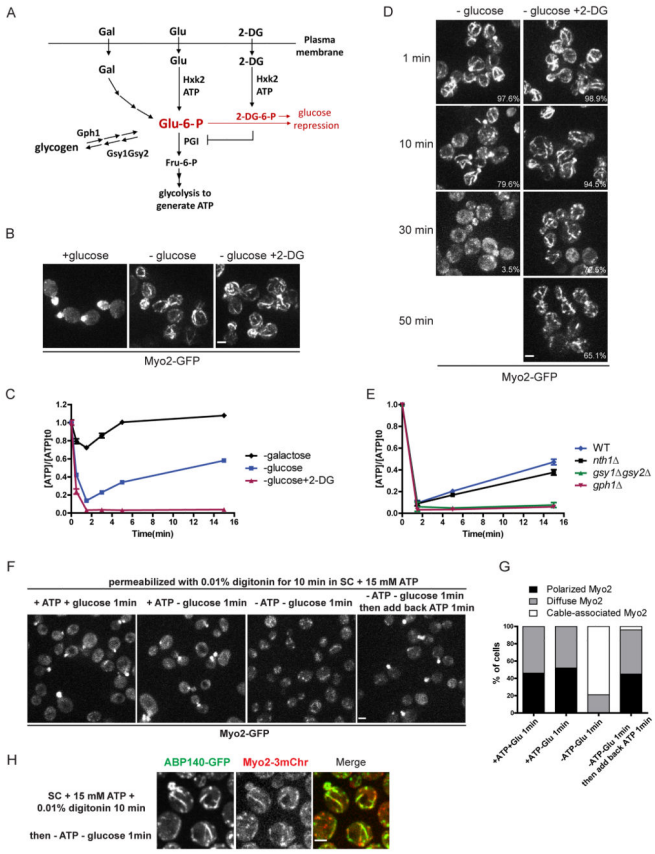

Figure 2. Myo2 localization correlates with intracellular ATP level

(A) Schematic diagram of the entry of glucose, galactose, 2-DG and glycogen into the glycolytic pathway in yeast cells.

(B) Cells grown in SC were transferred to fresh SC (left), SC lacking glucose (center) or SC with 2% 2-DG and no glucose (right).

(C) ATP levels in cells after glucose depletion (blue), galactose depletion (black) or glucose depletion and 2-DG addition (red). ATP concentrations are normalized to pre-starved cells. Error bars represent SD.

(D) Myo2-GFP in cells depleted of glucose with or without 2-DG after prolonged incubation. Percentage of cells containing Myo2 fibers is shown in the lower right corner. At least 200 cells were scored for each condition.

(E) ATP levels in cells after growth to early/mid-log phase in SC at times after glucose depletion. ATP concentrations are normalized to pre-starved cells. Error bars represent SD.

(F) Cells expressing Myo2-GFP were permeabilized as described in *Materials and Methods* and transferred to the conditions as indicated.

(G) Quantification of Myo2-GFP localization in (F). At least 200 cells were scored for each condition.

(H) Cells expressing Myo2-3mCherry and ABP140-GFP were permeabilized and depleted of glucose and ATP for 1 min. All scale bars, 2 μm.

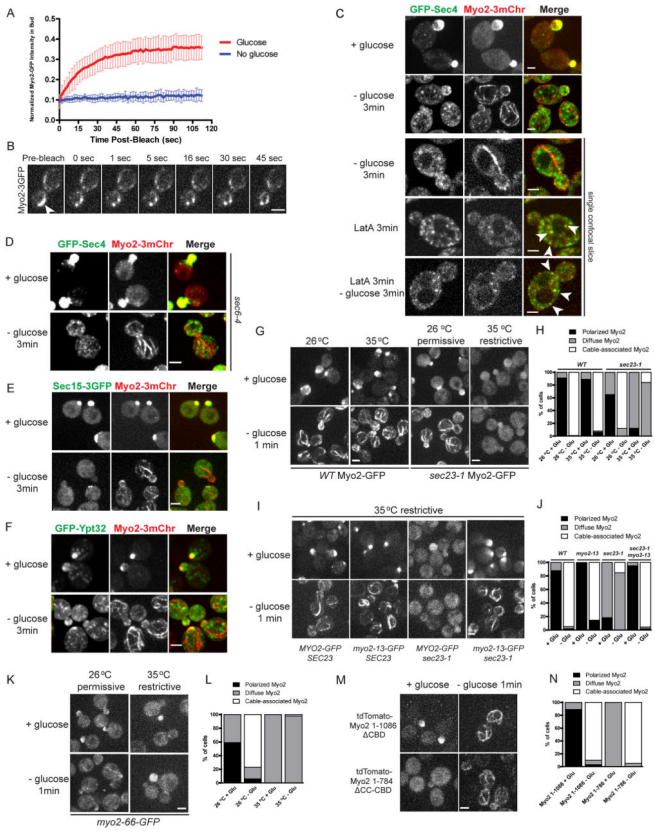

Figure 3. Myo2-mediated transport stops and Myo2 releases secretory cargo after glucose depletion

(A) Normalized Myo2-GFP intensity after photobleaching in the bud of cells incubated with fresh SC (red, n=17) or less than 10 min after glucose depletion (blue, n=16). Error bars represent SD.

(B) Frames from a movie showing photobleaching of a small region on cable-bound Myo2-3GFP in a glucose-depleted cell. Arrow indicates bleached area.

(C) Localization of Myo2-3mCherry and GFP-Sec4 in diploid cells grown in SC and transferred to fresh SC, SC lacking glucose for 3 min or pretreated with 120 μM LatA for 3 min and then transferred to fresh SC or SC lacking glucose with LatA. Arrows indicate examples of colocalization. See also Movie S2.

(D) *sec6-4* cells coexpressing Myo2-3mCherry and GFP-Sec4 were transferred to fresh SC or SC lacking glucose for 3 min.

(E–F) Cells coexpressing Myo2-3mCherry and Sec15-3GFP (E) or GFP-Ypt32 (F) were transferred to fresh SC or SC lacking glucose for 3 min.

(G) Localization of Myo2-GFP in WT or *sec23-1* pre-incubated at 26 °C or 35 °C for 45 min, transferred to fresh SC or SC lacking glucose equilibrated to pre-incubation temperature.

(H) Quantification of Myo2-GFP localization in (G). At least 150 cells were scored for each condition.

(I) Localization of Myo2-GFP and Myo2-13-GFP in *SEC23* and *sec23-1* cells pre-incubated at 35°C for 45 min and transferred to prewarmed SC or SC lacking glucose for 1 min.

(J) Quantification of Myo2-GFP localization in (I). At least 150 cells were scored for each condition.
(K) Localization of Myo2-66-GFP in cells pre-incubated at 26 °C or 35 °C for 45 min, transferred to SC or SC lacking glucose at pre-incubated temperature for 1 min.
(L) Quantification of Myo2-GFP localization in (K). At least 100 cells were scored for each condition.
(M) Localization of tdTomato-Myo2-1-1086 (lacking cargo-binding domain) or tdTomato-Myo2-1-784 (lacking coiled-coil dimerization domain and cargo-binding domain) in the presence or absence of glucose.
(N) Quantification of Myo2-GFP localization in (N). At least 100 cells were scored for each condition. All scale bars, 2 μm.

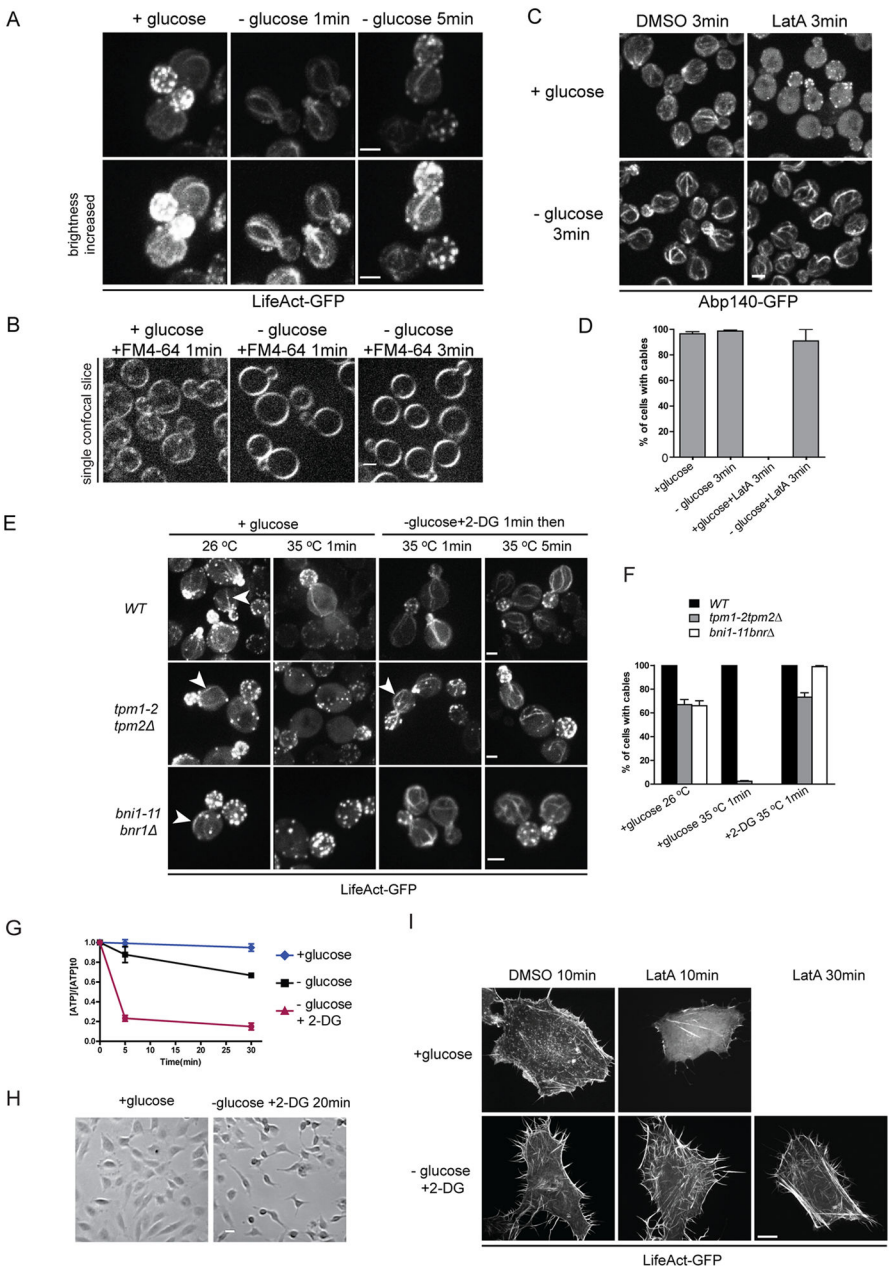

Figure 4. Changes in actin-based structures in ATP-deprived cells

(A) Cells expressing LifeAct-GFP grown in SC were transferred to fresh SC (left) or SC lacking glucose for 1 min (center) or 5 min (right). Lower panel shows the same pictures with brightness increased. See also Movie S3.

(B) Cells grown in SC were transferred to fresh SC or SC lacking glucose, 32 nM FM4-64 was added to the last wash of the medium change and incubated for indicated time.

(C) Cells expressing Abp140-GFP were transferred to fresh SC or medium lacking glucose supplemented with 120 μM LatA or equal volume of DMSO for 3 min. See also Figure S3B.

(D) Percentages of cells with actin cables in (C). At least 200 cells were scored for each condition. Error bars represent SD.

(E) WT, *tpm1-2tpm2*Δ or *bni1-11bnr1*Δ cells expressing LifeAct-GFP were transferred to fresh SC or SC with 2-DG but no glucose for 1 min and then shifted to 35°C. Arrows indicate examples of cables.

(F) Percentages of cells with actin cables in (E). At least 200 cells were scored for each condition. Error bars represent SD. (A–F) scale bars, 2 μm.

(G) ATP levels in HeLa cells transferred into DMEM with 0.45% glucose (blue), DMEM lacking glucose (black), or lacking glucose and supplemented with 0.45% 2-DG (red) at the indicated time points. ATP concentrations are normalized to pre-starved cells. Error bars represent SD.

(H) DIC images of HeLa cells after transfer to DMEM with 0.45% glucose (left) or DMEM with 0.45% 2-DG but no glucose (right) for 20 min. Scale bar, 50 μm.

(I) HeLa cells expressing LifeAct-GFP were transferred to DMEM with 0.45% glucose or DMEM with 0.45% 2-DG but no glucose for 10 min and then treated with 2.4 μM LatA. Representative images are shown in each condition except that no cells remained attached 30 min after LatA treatment in glucose-replete samples. Scale bar, 10 μm.